Electron Hydration in Pure Liquid Water. Existence of Two Nonequilibrium Configurations in the Near-Infrared Region

S. Pommeret, A. Antonetti, and Y. Gauduel*

Contribution from the Laboratoire d'Optique Appliquée, CNRS URA 1406, INSERM U275, Ecole Polytechnique-ENS Techniques Avancées, 91120 Palaiseau, France.
Received January 3, 1991. Revised Manuscript Received April 5, 1991

Abstract: Time-dependent absorption spectroscopy of photogenerated electrons in pure liquid water has been performed in the near-infrared region (near-IR) using femtosecond optical pulses. Time-resolved data are analyzed by considering the formation of nonequilibrium electronic states and fully relaxed hydrated electrons (ground state). In the spectral range 805–880 nm, femtosecond kinetics exhibit an early significant relaxation. A two-state activated model combined with an early recombination phenomenon between hydrated electrons and prototropic species precludes the existence of an isosbestic point. Furthermore, spectroscopic data in the near-infrared exhibit an additional component which is built up with a time constant of 130 ± 20 fs and whose lifetime equals 330 ± 20 fs. The data provide strong evidence that the early relaxation seen in the near-IR (around 820 nm) cannot be assigned to the geminate recombination but rather to an ultrafast single-electron-transfer reaction. This process would involve a population of excess electrons which undergoes a hydration process in the solvation shell of a hydronium ion (H_3O^+) or a hydroxyl radical (OH). The resulting encounter pair (e^-:H_3O^+:OH)$_{nH_2O}$ exhibits a cleavage rate of 3×10^{12} s^{-1}. It is suggested that structural cooperative effects linked to the presence of prototropic species would favor a charge separation channel equivalent to a low-energy photochemical process. In this hypothesis, the trapping of photogenerated electrons would occur in the transient cage involving prototropic species (H_3O^+, OH) and a few water molecules.

Introduction

Understanding of solvent effects during charge-transfer reactions must be based on detailed information on the solvation dynamics of elementary charges (epithermal electron, for instance) or the time-dependent Stokes shift of molecular probes in polar liquids.[1-13] Experimental and theoretical studies of electrons in polar media constitute an active area of research to elucidate the type and location changes induced by a charge separation, the role of the local electron–solvent interactions, and the molecular process associated with the solvent relaxation around an excess electron.[14-32] Indeed, quantum statistical studies using path integral molecular dynamics and Monte Carlo statistical methods have permitted considerable progress on equilibrium structure, optical spectroscopy, and relaxation dynamics of hydrated electrons (e^-_{hyd}).[20,21,24,28]

The investigations on the primary events linked to the hydration of photogenerated electron in aqueous media have been performed using femtosecond laser pulses and absorption spectroscopic methods.[33-36] In pure liquid water at 294 K, the experimental data obtained at different test wavelengths in the spectral range 520–1250 nm have permitted us (i) to reconstruct transient spectra between 0 and 2 ps and (ii) to investigate the time dependence of the signal assigned to different electronic state configurations. The spectral trace of the fully hydrated electron is entirely developed in less than 2×10^{-12} s.[33] The structureless character of the broad band (E_{max} = 1.7 eV) is comparable to the spectral trace of the hydrated electron generated by pulse radiolysis or picosecond photolysis.[14,17,37] Considering the time-dependent spectra of photogenerated electrons in pure water, we suggested a few years ago that the hydration process occurs mainly through a transition between trapped electron (prehydrated electron: e^-_{prehyd}) and equilibrium configuration (ground state of the fully hydrated state).[33,34] In this way a two-state activated kinetic process has been proposed for which the early-infrared band seen at the femtosecond time scale was assigned to the existence of a precursor of the fully hydrated state (presolvated state). The infrared electron appears with a global time T_1 of 110 fs, and its relaxation follows a monoexponential law characterized by a time constant T_2 (240 fs). However, the fact that our femtosecond spectroscopic experiments do not imply the existence of a well-defined isosbestic point would suggest that small spectral fluctuations or additional spectral components in the near-infrared region can influence the time-dependent absorption spectrum of excess electrons in water. This femtosecond spectral information permitted us to conclude that, during the electron hydration

* To whom correspondence should be addressed.

(1) Rentzepis, P. M.; Jones, R. P.; Jortner, J. J. *J. Chem. Phys.* **1973**, *59*, 766.
(2) Chase, W. J.; Hunt, J. W. *J. Phys. Chem.* **1975**, *79*, 2835.
(3) Wiesenfeld, J. M.; Ippen, E. P. *Chem. Phys. Lett.* **1980**, *73*, 47.
(4) Huppert, D.; Kenney-Wallace, G. A.; Rentzepis, P. M. *J. Chem. Phys.* **1981**, *75*, 2265.
(5) Gauduel, Y.; Migus, A.; Martin, J. L.; Antonetti, A. *Chem. Phys. Lett.* **1984**, *108*, 318.
(6) Castner, E. W.; Fleming, G. R.; Bagchi, B. J. *J. Chem. Phys.* **1988**, *89*, 3519.
(7) Maroncelli, M.; Castner, E. W.; Bagchi, B.; Fleming, G. R. *Faraday Discuss. Chem. Soc.* **1988**, *85*, 199.
(8) Williams, R. J. P. *Biochem. Int.* **1989**, *18*, 475.
(9) Jarzeba, W.; Walker, G. C.; Johnson, A. E.; Kahlow, M. A.; Barbara, P. F. *J. Phys. Chem.* **1988**, *92*, 7039.
(10) Bagchi, B.; Oxtoby, D. W.; Fleming, G. R. *Chem. Phys.* **1984**, *86*, 257.
(11) Chandra, A.; Bagchi, B. *J. Phys. Chem.* **1990**, *94*, 1874.
(12) Bagchi, B. *Annu. Rev. Phys. Chem.* **1989**, *40*, 115.
(13) Simon, J. D.; Su, S. G. *J. Chem. Phys.* **1987**, *87*, 7016.
(14) Hart, E. J.; Anbar, M. *The Hydrated Electron*; Wiley Intersciences: New York, 1970.
(15) Baxendale, J. H. *Can. J. Chem.* **1977**, *78*, 1996.
(16) Kenney-Wallace, G. A.; Jonah, C. D. *J. Phys. Chem.* **1982**, *86*, 2572.
(17) Nikogosyan, D. N.; Oraevsky, A. O.; Rupasov, V. I. *Chem. Phys.* **1983**, *77*, 131.
(18) Calef, D. F.; Wolynes, P. G. *J. Phys. Chem.* **1983**, *87*, 3387.
(19) Suzman, L. D.; Helman, A. B. *Chem. Phys. Lett.* **1985**, *114*, 301.
(20) Schnitker, J.; Rossky, P. J.; Kenney-Wallace, P. J. *J. Chem. Phys.* **1986**, *85*, 2926.
(21) Jonah, C. D.; Romero, C. *Chem. Phys. Lett.* **1986**, *123*, 209.
(22) Laria, D.; Chandler, D. *J. Chem. Phys.* **1987**, *87*, 4088.
(23) Landman, U.; Barnett, R. N.; Cleveland, C. L.; Scharf, D.; Jortner, J. *J. Phys. Chem.* **1987**, *91*, 4890.
(24) Schnitker, J.; Rossky, P. J. *J. Chem. Phys.* **1987**, *86*, 3462.
(25) Wallqvist, A.; Martyna, G.; Berne, B. J. *J. Phys. Chem.* **1988**, *92*, 1721.
(26) Sprik, M.; Klein, M. L. *J. Chem. Phys.* **1988**, *89*, 1592.
(27) Hilczer, M.; Bartczak, W. M.; Kroh, J. *J. Chem. Phys.* **1988**, *89*, 2286.
(28) Motakabbir, K. A.; Rossky, P. J. *Chem. Phys.* **1989**, *129*, 253 and references therein.
(29) Romero, C.; Jonah, C. D. *J. Chem. Phys.* **1989**, *90*, 1877.
(30) Bartczak, W. M.; Hilczer, M.; Kroh, J. *J. Phys. Chem.* **1987**, *91*, 3834. Hilczer, M.; Bartczak, W. M.; Sopek, M. *Radiat. Phys. Chem.* **1990**, *36*, 199.

0002-7863/91/1513-9105$02.50/0

phenomenon, the contribution of a continuous shift from the near-infrared to the visible is not significant.[33,36] This conclusion does not agree with current theoretical treatment of electron solvation including the dielectric model or mean spherical approximation (MSA).[18,19,38-42]

Recent experimental investigations in pure liquid water have suggested that electron hydration can be understood as an internal conversion process and supported the existence of an isosbestic point at 820 nm.[43] Theoretical studies using hole-burning molecular dynamics simulations (MD) suggest that, in the two-photon generation of excess electrons in pure liquid water, the majority of the excess electron population will be localized in transient configurations (trapped state or excited hydrated electron) and would undergo an internal transition (nonadiabatic transition) toward the fully hydrated electron (ground state).[31,45] In pure liquid water, the view of the electron solvation as an internal conversion process remains an open question because up to now no experimental investigation has been performed in detail at short (t = 2 ps) and long times (t > 10 ps) in the suspected isosbestic spectral range 800–880 nm.[33] During the electron solvation process, an isosbestic point can be demonstrated if the primary step supports only a two-state activated model such as internal conversion or radiationless transition, i.e., a unique physical process. That means that, in the specific case of femtosecond photoionization of pure liquid water, two populations of electrons exhibiting significant spectral differences in the visible and the near-infrared regions would be generated. Theoretical investigations of Messmer and Simon[32] on electron trapping and solvation in pure liquid water are partially consistent with our experimental spectral data and suggest that different populations of nonequilibrium electronic configurations (prehydrated states, excited solvated state, and trapped electron by preexisting deep traps) can contribute to the infrared signal before the electron reaches equilibrium (hydrated state). In such conditions the computed simulations show that no isosbestic point can be really observed.

The aim of this paper is to present new experimental results on femtosecond near-infrared spectroscopy to extend the understanding of time-dependent spectra of photogenerated electrons in pure liquid water. In the investigated spectral range (805–880 nm), in order to carefully explore the time-dependent absorption dynamics of photogenerated electrons in pure liquid water, it is necessary to consider additional data on the physicochemical steps subsequent to the initial energy deposition in the polar fluid. Following femtosecond photoionization of water molecules, several early events have been recently investigated in the first picoseconds (t < 10 ps): an ultrafast water cation reaction with water molecules ($H_2O^+ + H_2O$), a relaxation of infrared electrons toward equilibrium configurations, and recombination of hydrated electrons with prototropic species ($H_3O^+ + OH$).[44,46,47] In this way,

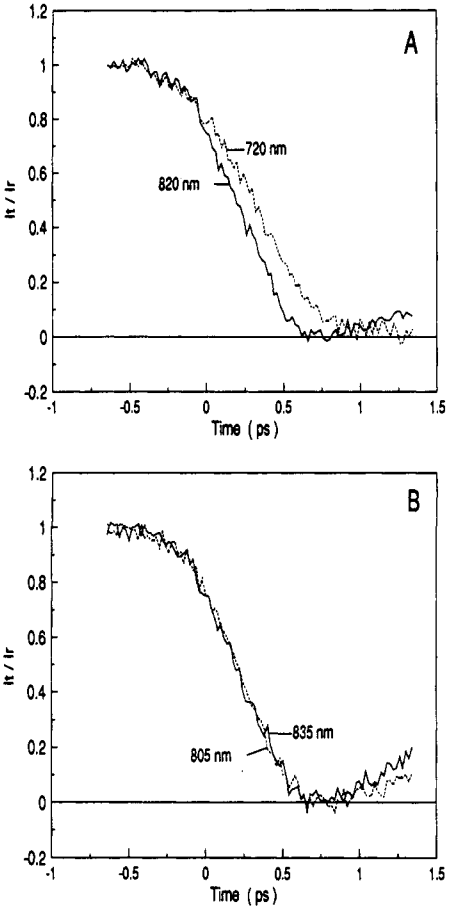

Figure 1. Rise time of the induced absorption in the red and the near-infrared spectral regions following the femtosecond photoionization of neutral water molecules by ultraviolet pulses (310 nm) at 294 K. Test wavelengths: (A) 720 and 820 nm; (B) 805 and 835 nm. In the near-IR an early relaxation can be observed.

we will focus our attention on the kinetic data at short (t < 2 ps) and long times (t > 10 ps) in the near-infrared spectral region (near-IR), considering the existence of an early geminate recombination reaction between the hydrated electrons and prototropic species (hydronium ion and hydroxyl radical). We will describe whether several nonequilibrium configurations are involved in the time-dependent spectra of photogenerated electrons in pure liquid water.

Experimental Section

Femtosecond spectroscopic experiments were performed at 294 K in a continuously vibrating fixed-volume Suprasil cell (2-mm path length) so that using a laser pulse repetition rate of 10 Hz causes each laser pulse to excite a new region of the sample. Bideionized water was doubly distilled with $KMnO_4$ (resistivity greater than 17 MΩ at 294 K, pH 6.45) in a quartz still. Oxygen was removed from the samples by tonometry using pure nitrogen gas.

The femtosecond absorption spectroscopy apparatus has been described in detail previously.[34a,48] The photoionization of solvent molecules or the chromophore is induced by femtosecond ultraviolet pulses (λ_p = 310 nm, E = 4 eV, I = 10^{11} W cm^{-2}) obtained by focusing an amplified 620-nm beam into a 1.5-mm KDP crystal. A continuum produced by the femtosecond laser provides the probe, tunable test, and reference beams. For a given wavelength the signals corresponding to the probe and reference pulse energies are transferred to a HP computer and stored on disk for further processing. Because of the large spectral region under investigation, the group velocity dispersion of the continuum induces an important shift temporal overlap between the pump and the probe beams. Therefore, careful experiments were conducted at each

(31) Barnett, R. B.; Landman, U.; Nitzan, A. *J. Chem. Phys.* **1989**, *90*, 4413.
(32) Messmer, M. C.; Simon, J. D. *J. Phys. Chem.* **1990**, *94*, 1220.
(33) Gauduel, Y.; Martin, J. L.; Migus, A.; Antonetti, A. In *Ultrafast Phenomena*; Fleming, G. R., Siegman, A. E., Eds.; Springer-Verlag: New York, 1986; Vol. V, p 308. Migus, A.; Gauduel, Y.; Martin, J. L.; Antonetti, A. *Phys. Rev. Lett.* **1987**, *58*, 1559.
(34) (a) Gauduel, Y.; Migus, A.; Antonetti, A. In *Chemical Reactivity in Liquid; Fundamental Aspects*; Moreau, M., Turcq, P., Eds.; Plenum Press: New York, 1988; pp 15–32; (b) *Radiat. Phys. Chem.* **1989**, *34*, 5.
(35) Long, F. H.; Lu, H.; Eisenthal, K. B. *Chem. Phys. Lett.* **1989**, *160*, 464.
(36) Gauduel, Y.; Pommeret, S.; Migus, A.; Yamada, N.; Antonetti, A. *J. Opt. Soc. Am. B: Opt. Phys.* **1990**, *7*, 1528.
(37) Jou, F. Y.; Freeman, G. R. *J. Phys. Chem.* **1979**, *83*, 2383.
(38) Mozumder, A. *Radiat. Phys. Chem.* **1988**, *32*, 287 and references therein.
(39) Schiller, R. *Chem. Phys. Lett.* **1970**, *5*, 176.
(40) Kivelson, D.; Friedman, H. *J. Phys. Chem.* **1989**, *93*, 7026.
(41) Wolynes, P. *J. Chem. Phys.* **1987**, *86*, 5133.
(42) Rips, I.; Klafter, J.; Jortner, J. *J. Chem. Phys.* **1988**, *88*, 3246.
(43) Long, F. H.; Lu, H.; Eisenthal, K. B. *Phys. Rev. Lett.* **1990**, *64*, 1469.
(44) (a) Gauduel, Y.; Pommeret, S.; Migus, A.; Antonetti, A. *Chem. Phys.* **1990**, *149*, 1; (b) *J. Phys. Chem.* **1991**, *95*, 533.
(45) Rossky, P. J.; Schnitker, J. *J. Phys. Chem.* **1988**, *92*, 4277.
(46) Lu, H.; Long, F. H.; Bowman, R. M.; Eisenthal, K. B. *J. Phys. Chem.* **1989**, *93*, 27.
(47) Gauduel, Y.; Pommeret, S.; Migus, A.; Antonetti, A. *J. Phys. Chem.* **1989**, *93*, 3880.
(48) Migus, A.; Antonetti, A.; Etchepare, J.; Hulin, D.; Orszag, A. *J. Opt. Soc. Am. B: Opt. Phys.* **1985**, *B2*, 584.

wavelength to determine the zero-time delay and the time response function of the apparatus. The precise procedures used to obtain the position of the zero-time delay have been described in detail elsewhere.[34a] Additional measurements have been performed to determine the influence of the polar media on the shift of the zero. In this procedure, for each test wavelength, the Suprasil cell containing the sample is localized on the probe and reference beams before the pump pulse.

The theoretical studies on time-dependent absorption spectra of excess electrons in liquid water have been performed on a Sparc Station 1+ (Sun OS 4-0-3).

Results and Discussion

1. Time Dependence of Induced Absorbance in the Visible and Near-IR. Figure 1 summarizes the results of a set of experiments which have been performed in the visible and the near-IR spectral regions. Comparison of the curves obtained at 720 and 820 nm (Figure 1A) shows the existence of an early relaxation in the near-infrared region. Similar initial relaxations have been observed for different test wavelengths around 820 nm (Figure 1B).

Considering these experimental data, the important points to examine are (i) the influence of the early electron–radical pair recombination on the time dependence of the spectrum and the existence of an isosbestic point and (ii) the meaning of an early relaxation in the near-IR.

To answer the first question, we have performed computed simulations examining the influence of early one-dimensional random walk reaction dynamics (T_d) on the rise time and behavior of the induced absorption in the red (720 nm) and near-infrared (820 nm) spectral regions. The computed fits have been performed with a kinetic model which considers (i) that the electron solvation process occurs through a single transition between the trapped and fully hydrated species, i.e., a two-state activated process, and (ii) the early behavior of the hydrated electron, i.e., geminate recombination of hydrated electron with H_3O^+ or OH.[44,47]

For the alternative test wavelengths, the induced absorption rise time has been analyzed considering the convolution of the pump–probe pulses with the expected signal rise dynamics due to electron trapping and solvation and the early electron–radical pair recombination. The rise time of the normalized induced absorption in the red spectral region ($\Delta\alpha^{\omega}(\tau)$) consists of the linear combination of two populations of hydrated electrons: one assigned to a long-lived hydrated electron $(e^-_{hyd})_{nrecomb}$ and the other one to a hydrated electron population performing an early recombination $(e^-_{hyd})_{recomb}$.

$$\Delta\alpha^{\omega}_{Tot}(t) = (1-\gamma)\Delta\alpha^{\omega}_{(e^-_{hyd})_{nrecomb}}(t) + \gamma\Delta\alpha^{\omega}_{(e^-_{hyd})_{recomb}}(t) \quad (1)$$

To study the effect of an ultrafast geminate recombination, we have considered a model in which an initial electron–radical pair ($H_3O^+\cdots e^-_{hyd}$ or $OH\cdots e^-_{hyd}$) executes a reaction following a 1D walk (eqs 2 and 3). This model includes the fact that at short time ($t < 10^{-10}$ s) a fraction of the photogenerated electrons are hydrated in the vicinity of the hydronium ion or the hydroxyl radical.

$$H_3O^+ + e^-_{hyd} \rightarrow H + H_2O \quad (2)$$

$$OH + e^-_{hyd} \rightarrow OH^- \quad (3)$$

A recombination process controlled by 1D diffusion can be modeled using the analytical expression $N_{e^-_{hyd}}(t) = \gamma N^{\circ}_{e^-_{hyd}}\,\mathrm{erf}\,(T_d/t)^{1/2}$, in which γ represents the fraction of the population of hydrated electrons ($N^{\circ}_{e^-_{hyd}}$) that will recombine, and T_d the jump time of the recombination. This kinetic model implies that the recombination length represents the jump distance occurring with a frequency λ.[47]

Over an ultrashort time scale (2 ps full scale), the influence of the early recombination process on the rise time and behavior of the signal is represented in Figure 2A. The best fit is obtained for a 55% geminate recombination. The figure indicates that the early recombination process cannot be observed on a short time scale (2 ps full scale). At a longer time, the relaxation due to electron–radical pair recombination is still well fitted with a curve which considers the fraction of the initial hydrated electron population involved in this fast recombination process (Figure 3).

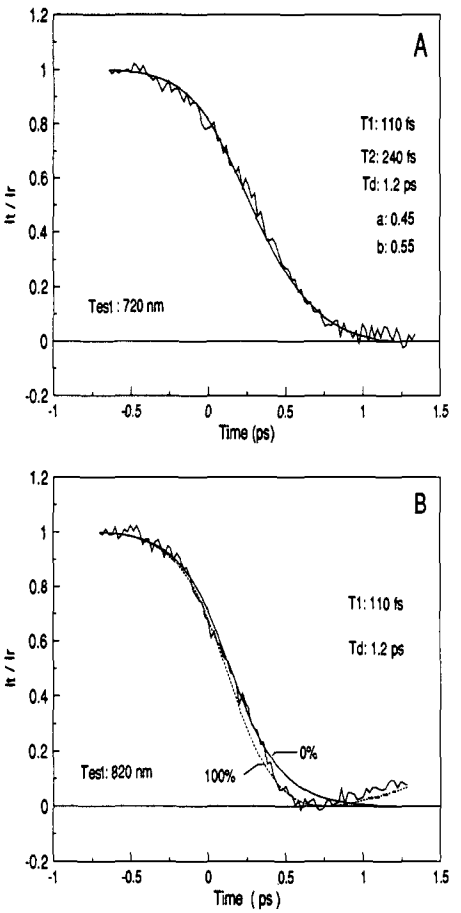

Figure 2. Influence of an early electron pair recombination on the appearance time and early behavior of a signal. (A) At 720 nm the signal is assigned to the formation of hydrated electrons following two characteristic times: the trapping and solvation times equal to 110 and 240 fs, respectively.[33] The smooth line represents the best computed fit involving the combination of the appearance time of the hydrated electron and the early geminate recombination through a random-walk law (erf $(T_d/t)^{1/2}$) with T_d = 1.2 ps and 55% of recombination. (B) In the near-IR (820 nm), the experimental trace is represented with different computed fits including the existence of an isosbestic point appearing with the constant time T_1 = 110 fs and the influence of an ultrafast recombination between hydrated electron and prototropic species (0 or 100% of relaxation); the relaxation occurs following a random-walk law as previously defined at 720 nm.

To analyze the experimental data obtained at 820 nm (Figures 2B and 3), let us consider, at this stage, the theoretical treatment of an isosbestic point for a two-state activated model. As previously shown in our papers,[33,34] the kinetic model of electron hydration implies the existence of an intermediate state (A_1 or e^-_{prehyd}) absorbing in the infrared and corresponding to a precursor of the fully hydrated state (A_2 or e^-_{hyd}):

$$A_0 \xrightarrow[\epsilon_1]{T_1} A_1 \xrightarrow[\epsilon_2]{T_2} A_2 \quad (4)$$

Starting from an initial virtual species created instantaneously (an excited state of water molecules), we have assumed the existence of two separate species during the electron hydration process. One species, absorbing in the infrared (e^-_{prehyd}), corresponds to a nonequilibrium configuration which is built up with a time constant T_1 (trapping rate constant = $k_1 = 1/T_1 = 9 \times 10^{12}$ s^{-1}).[33] This nonequilibrium electronic configuration then relaxes toward the fully hydrated state (e^-_{hyd}) following first-order kinetics with a time constant T_2 (solvation rate = $k_2 = 1/T_2 = 4 \times 10^{12}$ s^{-1}). In this kinetic scheme, the analysis of the time-resolved spectroscopic data considers the convolution of the pump–probe pulse temporal profile and the expected signal rise dynamics for each test wavelength. The signal is the linear

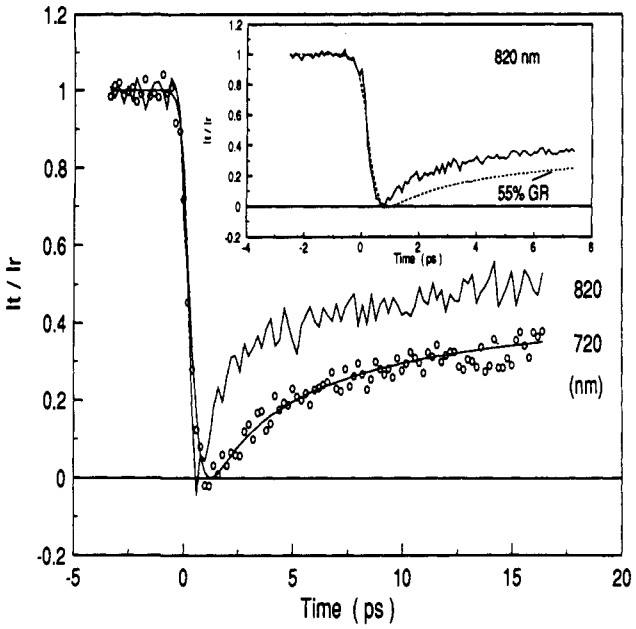

Figure 3. Early behavior of the induced absorption at 720 and 820 nm following the femtosecond ultraviolet photoionization of water molecules. In the red spectral region, the smooth line represents the best computed random-walk law (erf $(T_d/t)^{1/2}$) with T_d = 1.2 ps and 55% of electron–radical pair recombination. The inset shows the detail of time-resolved data at 820 nm (10 ps) with the representation of a computed curve involving the existence of an isosbestic point and a subsequent partial relaxation (55%) due to an electron–radical pair recombination following a random-walk law (T_d = 1.2 ps).

combination of the different transient species $A_1(t)$ and $A_2(t)$, with ϵ_1 and ϵ_2 the extinction coefficients of A_1 and A_2, respectively.

$$\Delta\alpha^{\omega}(t) = l(\epsilon_1{}^{\omega}A_1(t) + \epsilon_2{}^{\omega}A_2(t)) = A_0\epsilon_1{}^{\omega}\frac{T_2}{T_2 - T_1}\left[\exp\left(-\frac{t}{T_2}\right) - \exp\left(-\frac{t}{T_1}\right)\right] + A_0\epsilon_2{}^{\omega}\left(1 - \frac{1}{T_2 - T_1}\right)\left[T_2\exp\left(\frac{-t}{T_2}\right) - T_1\exp\left(\frac{-t}{T_1}\right)\right] \quad (5)$$

In eq 5, A_0 represents an initial population of quasi-free electrons. Regardless of the test wavelength, the expression can be written as follows:

$$\Delta\alpha(t) = A_0\left[\epsilon_2 + (\epsilon_1 - \epsilon_2)\left(\frac{T_2}{T_2 - T_1}\right)\exp\left(\frac{-t}{T_2}\right) + \frac{\epsilon_2T_1 - \epsilon_1T_2}{T_2 - T_1}\exp\left(\frac{-t}{T_1}\right)\right] \quad (6)$$

If $\epsilon_1 = \epsilon_2$, i.e., at the isosbestic point, then

$$\Delta\alpha(t) = A_0\epsilon_2 + \left(\frac{\epsilon_2T_1 - \epsilon_1T_2}{T_2 - T_1}\right)\exp\left(\frac{-t}{T_1}\right) = A_0\epsilon_2\left(1 - \exp\left(\frac{-t}{T_1}\right)\right) \quad (7)$$

The expression (7) means that, at the isosbestic point, the signal is built up with a single rise time and is characterized by a long lifetime as long as the total concentration of photogenerated electrons remains constant (absence of ultrafast recombination, for instance).

Figure 2B represents the experimental trace we have obtained at 820 nm with a theoretical curve defined by eq 7. The comparison between computed fit and the experimental curve clearly demonstrates that the apparent rise time of the signal at 820 nm cannot be fitted to a single time constant. Additional computed fit shows the influence of an early electron–radical pair. Even if we consider that the total relaxation of the signal occurs through a recombination process, no fit agrees with the experimental data at short and long times (Figure 3). From this figure, it is clear that a component characterized by a fast relaxation time exists in the near-infrared; such a component is not observed in the red spectral region. Consequently, the early decay we observe around 820 nm cannot be explained by a contribution of the early electron–radical pair recombination. Moreover, the percentage of the signal decay after 15 ps is more important in the near-IR than at 720 nm (Figure 3). These observations raise the second important point, which concerns the exact meaning of an isosbestic point when the second population (here the ground state of hydrated electron) is not stabilized at short time ($t \ll 10$ ps). This key point is discussed in the following section.

2. Early Geminate Recombination and Transient Absorption Spectra. To analyze the influence of an early reactivity of hydrated electron on the time dependence induced absorption in the near-infrared, we have performed simulations on the transient spectra data in pure liquid water. For each test wavelength the temporal evolution of the signal $\Delta\alpha^{\omega}(\tau)$ is calculated from the value of molecular extinction coefficient for prehydrated and hydrated electrons. Optical absorption data for the hydrated electrons are derived from experimental investigations of Jou and Freeman.[37] These data inferred Gaussian/Lorentzian shape functions with E_{Amax} = 1.75 eV, W_r = 0.34, and W_b = 0.48 eV ($W_{1/2}$ = 0.83 eV). The absorption band of the infrared electron (prehydrated state) was assigned a maximum at 1600 nm (E_{Amax} = 0.77 eV)[45] and a Gaussian bandwidth of 0.6 eV. For a pure two-state activated process the transient spectra is reconstructed considering the contribution of the two spectral bands.

The simulations of the time-resolved data have been carefully conducted with a kinetic model, which takes into account the convolution of the pump–probe pulse temporal profile and the expected signal rise dynamics including all the different transient species. More precisely, the induced absorbance at a specific frequency (ω) and for a time delay (τ) between the excitation and the probe pulses is the sum of the contribution $\alpha_i{}^{\omega}(\tau)$ of all the species:

$$\Delta\alpha^{\omega}(\tau) = \sum\alpha_i{}^{\omega}(\tau) = \sum C_i\epsilon_i{}^{\omega}l \quad (8)$$

In the case of a small signal, the evolution of the different populations during the pumping and probing follows the relationship

$$\Delta\alpha_i{}^{\omega}(\tau) = \epsilon_i{}^{\omega}l\int_{-\infty}^{+\infty} C_i(\tau - \tau')\, C^{\omega}(\tau')\, d\tau' \quad (9)$$

with $C^{\omega}(\tau')$ the normalized correlation between the probe and the pump pulse:

$$C^{\omega}(\tau') = \int_{-\infty}^{+\infty} I_1(t + \tau')\, I_p{}^2(t)\, dt \quad (10)$$

In these expressions, l is the interaction length and ϵ^{ω} and C_i, respectively, are the molar extinction coefficient and the concentration of species i.

The total absorbance of the test pulse $\Delta\alpha^{\omega}(\tau)$ is described by an expression which considers the evolution of the different electron populations during the excitation and probe pulses (e^-_{prehyd} and e^-_{hyd}):

$$\Delta\alpha^{\omega}(\tau) = \Delta\alpha^{\omega}{}_{e^-_{prehyd}}(\tau) + \Delta\alpha^{\omega}{}_{e^-_{hyd}}(\tau) \quad (11)$$

The different spectral contributions are defined as follows:

$$\alpha^{\omega}{}_{e^-_{prehyd}}(\tau) = \epsilon^{\omega}{}_{e^-_{prehyd}}l\int_{-\infty}^{+\infty} C_{e^-_{prehyd}}(\tau - \tau')\, C(\tau')\, d\tau' \quad (12)$$

$$\alpha^{\omega}{}_{e^-_{hyd}}(\tau) = \epsilon^{\omega}{}_{e^-_{hyd}}l\int_{-\infty}^{+\infty} C_{e^-_{hyd}}(\tau - \tau')\, C(\tau')\, d\tau' \quad (13)$$

In these expressions, $\epsilon^{\omega}{}_{e^-_{prehyd}}$ ($\epsilon^{\omega}{}_{e^-_{hyd}}$), $C_{e^-_{prehyd}}(t)$, and $C_{e^-_{hyd}}(t)$ are the molar extinction coefficient and the time-dependent concentrations of the prehydrated and hydrated electrons, respectively.

The first population, assigned to the infrared electron, appears with a time constant T_1 and decay T_2. The concentration $C_{e^-_{prehyd}}$ at a time t follows the expression

$$C_{e^-_{prehyd}}(t) = C^{\circ}{}_{e^-_{prehyd}}[T_2/(T_2 - T_1)][\exp(-t/T_2) - \exp(-t/T_1)] \quad (14)$$

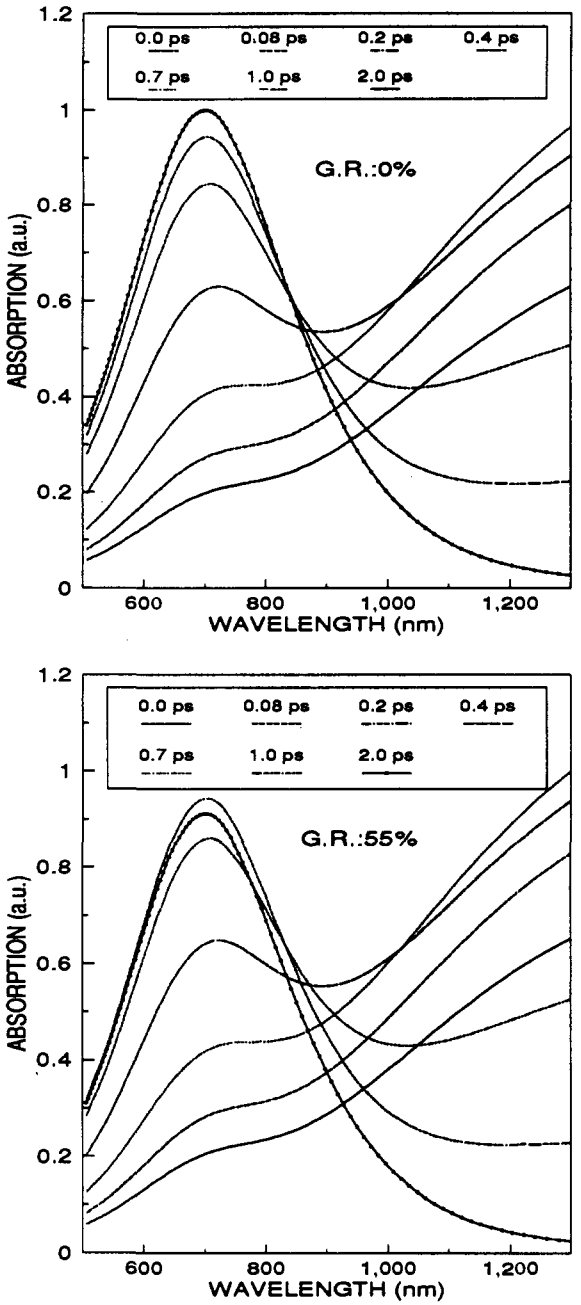

Figure 4. Computed simulation of transient spectra of excess electrons in pure liquid water. This simulation considers the existence of a two-state activated process at 294 K. Upper part: The simulation is performed by neglecting the existence of an early electron–radical pair recombination (GR=0%). An isosbestic point would be theoretically observed around 850 nm. Lower part: An early geminate recombination involving fully hydrated electrons and prototropic species (H_3O^+ or OH) is considered. A fraction of the hydrated electron population (GR=55%) will recombine with surrounding prototropic species following a process controlled by 1D diffusion (T_d = 1.2 ps). In this case, note the absence of an isosbestic point.

In eq 15, the time dependence of the population of hydrated electrons created at a time (t) includes the influence of the early geminate pair recombination

$$C_{e^-_{hyd}}(t) = \int_{-\infty}^{+t} \frac{dN_{e^-_{hyd}}(t)}{dt}\left(1 - \gamma \operatorname{erf}\left(\frac{T_d}{t - t'}\right)^{1/2}\right) dt' \quad (15)$$

with

$$N_{e^-_{hyd}}(t) = C^{\circ}_{e^-_{hyd}}[[1 - 1/(T_2 - T_1)][T_2 \exp(-t/T_2) - T_1 \exp(-t/T_1)]] \quad (16)$$

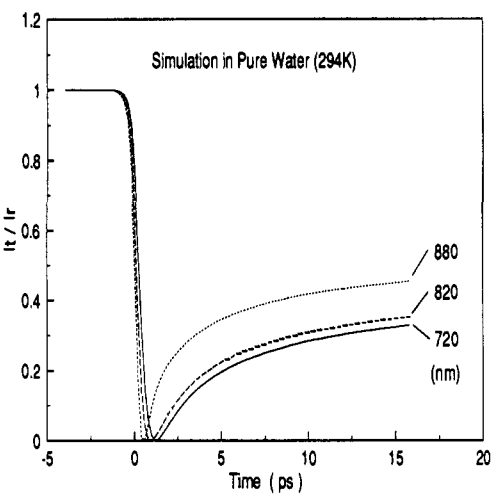

Figure 5. Computed simulations of the early decay behavior of a signal at 720, 820, and 880 nm. The kinetic data correspond to spectral simulations (see the bottom of Figure 4), i.e., a two-state activated process with an ultrafast geminate recombination of hydrated electron (GR=-55%).

The results of the simulations for a two-state activated process are represented in Figure 4. The upper part of the figure shows transient spectral data when the hydrated electrons do not react with prototropic species ($\gamma = 0$). It is interesting to notice that, in agreement with our experimental data in pure liquid water, a shoulder in the red spectral region exists at zero time. This means that it is not necessary to consider a direct electron capture by preexisting deep traps to describe this early visible component. The second information given by these simulations is that an isosbestic point would be theoretically observed around 840 nm. Although our spectral characteristics of the infrared (trapped) and visible (hydrated) electrons are not fully similar to those of Messmer and Simon,[24] the estimate on the position of this point remains comparable.

Data represented in Figure 4B show the influence of an early geminate recombination (55%) on the time-dependent absorption spectrum of excess electrons in pure liquid water at 294 K. The important information obtained by this simulation is that an isosbestic point cannot be obtained during the first 2 ps. This result is confirmed by the data reported in Figure 5. This figure represents the computed influence of an early geminate recombination on the behavior of the signal. At 720 nm, a two-state activated process combined with an early geminate recombination well fits the experimental trace as previously shown (Figure 3). However, the simulation exhibits no significant change on time-resolved data at 820 nm. Consequently, there is a discrepancy between the spectral simulations and the experimental data. Experimentally, the percentage and the dynamics of the signal decay at 820 nm are higher than at 720 nm.

3. Identification of an Additional Nonequilibrium Configuration in the Near-IR. Figure 6 represents the kinetic results obtained at 820 and 880 nm. Although the early relaxation dynamics are different, the percentage of the signal decay after 15 ps is similar at 820 and 880 nm (about 48% of relaxation). This observation cannot be entirely explained by a two-state activated process and an early recombination phenomenon because the longer the test wavelength the greater the early percentage of signal decay due to a contribution of prehydrated electrons. These experimental data bring quantitative support to the hypothesis that several photochemical channels are likely involved during the femtosecond photoejection of electrons from neutral water molecules. In alcohols, the existence of two channels for electron solvation has been previously identified at low and ambient temperature.[49]

In the specific case of pure liquid water, to analyze the time-dependent absorption in the near-IR (820–880 nm), we have

(49) Lewis, M. A.; Jonah, C. D. *J. Phys. Chem.* **1986**, *90*, 5367.

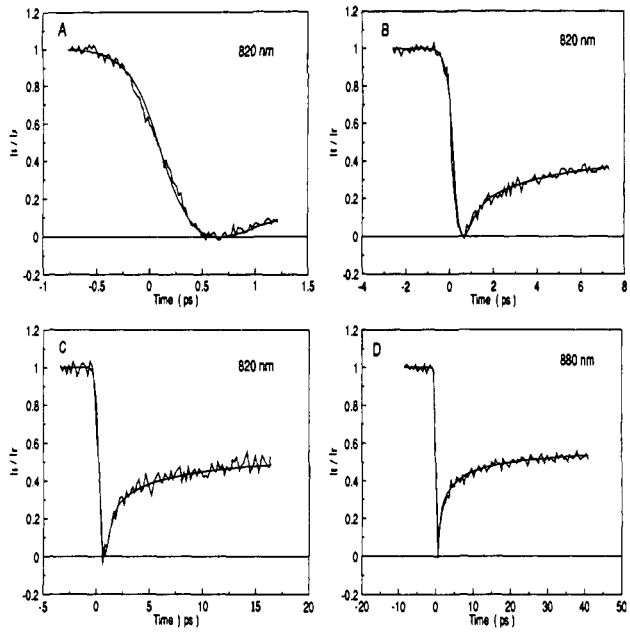

Figure 6. Time dependence of transient absorption in the near-IR (820 and 880 nm) following the femtosecond photoionization of water molecules at 294 K. The smooth lines represent the best fits. (A–C) The rise time of the signal results from the contribution of two processes: The electron hydration occurs through the formation of a localized prehydrated state with an appearance time of 110 fs and a subsequent relaxation in 240 fs; the second one is assigned to the formation of an encounter radical pair appearing in 130 fs and having a mean lifetime of 330 fs. (D) At 880 nm, the time dependence of the signal decay is assigned to the relaxation of trapped electrons toward a ground state of hydrated electrons considering a nonadiabatic process; the incomplete recovery of the signal is due to the contribution of a long-lived population of hydrated electrons.

considered the existence of a charge-transfer channel for which a fraction of the photogenerated electrons would be initially trapped within the solvation shells of the prototropic species (H_3O^+/OH), yielding an encounter pair

$$n H_2O + h\nu \longrightarrow (H_3O^+ \cdot\cdot OH)_{hyd} + e^-_{qf} \quad (k_3) \longrightarrow$$

$$[(H_3O^+ : e^- : OH)_{hyd} \longleftrightarrow (H_3O \cdot\cdot OH)^*_{hyd}] \quad (17)$$

$$[(H_3O^+ : e^- : OH)_{hyd} \longleftrightarrow (H_3O \cdot\cdot OH)^*_{hyd}] \quad (k_4) \longrightarrow H + H_2O$$

$$\longrightarrow H_3O^+ \cdots OH^-$$

$$\longrightarrow e^-_{hyd} + (H_3O^+ \cdots OH)$$

with $k_3 = 1/T_3$ and $k_4 = 1/T_4$.

The contribution of such a photochemical channel can explain the kinetic data obtained in the near-IR on short or long time scale (Figure 6A–C). At 820 nm, the computed best fits of the experimental trace assume that the encounter radical pair would occur with an appearance time (T_3) of 130 ± 20 fs and relax following a single transition state (monoexponential law) with a deactivation rate (T_4) of 330 ± 20 fs. The contribution of the signal due to this electron–radical pair equals about 30% at 820 nm. At a longer test wavelength (880 nm), the early signal decay can be assigned both to a contribution of this encounter pair and to prehydrated electrons (e^-_{prehyd}). However, at this test wavelength it is not easy to differentiate the exact contributions of the two nonequilibrium electronic states owing to the fact that the different times (T_1, T_2, T_3, and T_4) are very close.

Indeed, the resolution of kinetic data in the near-IR allows us to consider a specific photochemical channel in which the generation of excess electrons in pure liquid water can occur in the vicinity of prototropic species. In this context, we note that previous femtosecond investigations have demonstrated that in concentrated aqueous hydrochloric acid solution the high concentration of hydronium ion ($[H_2O/[HCl] = 5$) favors the localization of a significant fraction of excess electrons in the solvation shell of the cation $[(H_3O^+)_{nH_2O})]$; the probability P' that an excess electron is trapped inside the encounter volume is not negligible ($P' = 1 - \exp(-4\pi r_{eff}^3[S]/3 \times 10^3)) = 0.84$ for a r_{eff} of 3.41 Å. The concentration of the hydronium ion is defined by [S]. In these conditions, the spectral identification of an encounter pair has been obtained in the near-infrared ($E_{Amax} = 1.35$ eV).[50]

Ab initio calculations on the structural character of water molecules linked to the solvation shells of the hydronium ion in dilute solutions have shown that the radial distribution functions $g_{OO}(r)$ and $g_{OH}(r)$ exhibit maxima at 2.48 and 3.2 Å, respectively. At least two hydration shells can be considered over a 7-Å range.[51] Consequently, if an electron is directly trapped in the structured hydration shell of H_3O^+ or OH, the initial charge separation distance would be shorter than the Onsager radius ($r_c = 7$ Å in water) and very similar to the estimates of the reaction radius: $e^- \cdots H_3O^+ = 4.5$ Å, $e^- \cdots OH = 6$ Å.[52]

In pure liquid water, regarding the physical reasons for the existence of two photochemical channels, we must consider the photophysics of water molecules. Although several uncertainties remain about the estimate of the ionization potential of water molecules in the liquid phase, $I_{Liq} = IP_g + P^+ + V_0$, with IP_g the ionization potential in the gaseous phase, P^+ the adiabatic electronic polarization of the medium by the positive ion (H_2O^+), and V_0 the conduction band edge energy of the solvent. The existence of a low-dissociation channel for H_2O molecules has been suspected to compete with the direct ionization of the A^- state ($1b_1 \rightarrow 3sa_1$ for instance). Theoretically, the estimate of the energy required to generate electrons through vertical ionization (Born–Oppenheimer) is around 8.5 eV within the uncertainty about the value of V_0.[53,54] Experimentally, several works have suggested that the threshold energy for the formation of photogenerated hydrated electrons through one or two photons will be around 6.5 eV.[8,55,56] In our femtosecond photochemical experiments which use ultraviolet pulses ($E = 4$ eV) and high-energy density, the important point to discuss concerns the ionization process which can occur at energy lower than the vertical ionization threshold.

The electronic state achieved through a two-photon process below the theoretical ionization threshold (~8.5 eV) would correspond to ultrashort excited water molecules (Rydberg states for instance) for which an autoionization process in a condensed phase is possible. Previous studies conclude that a hydrated electron can be obtained when the excitation energy is lower than the energy band gap of water and suggest that an autoionization of water molecules would theoretically be feasible by a thermodynamic process with a free energy (ΔG) of 5.78 eV:[56,57]

$$2H_2O \rightarrow (H_3O^+)_{hyd} + (OH)_{hyd} + e^-_{hyd} \quad (18)$$

This charge transfer (eq 18) can be considered when the energy deposition occurs in favorable site geometry for which the thermodynamic process is made possible (low-energy photochemical channel). In this way the cooperative effect of two water molecules would enhance photogeneration of electrons on short distances; i.e., the trapping of the excess electron would occur in the first two solvation shells of the prototropic species.

The intermediate state of this photochemical channel would correspond to an autoionization of excited water molecules within a hydrogen-bonded lattice, yielding a very fast proton transfer from H_2O^+ to its nearest neighbors through few vibrational periods. In pure liquid water, this process would compete with the other electron solvation channels (Figure 7). Recent investigations of primary events triggered by femtosecond ultraviolet pulses

(50) Gauduel, Y.; Pommeret, S.; Migus, A.; Yamada, N.; Antonetti, A. *J. Am. Chem. Soc.* **1990**, *112*, 2925.
(51) Fornili, S. L.; Migliore, M.; Palazzo, M. A. *Chem. Phys. Lett.* **1986**, *125*, 419.
(52) Turner, J. E.; Hamm, R. N.; Wright, H. A.; Ritchie, R. H.; Magee, J. L.; Chatterjee, A.; Bolch, W. E. *Radiat. Phys. Chem.* **1988**, *32*, 503.
(53) Grand, D.; Bernas, A.; Amouyal, E. *Chem. Phys.* **1979**, *44*, 73.
(54) Delahay, P. *Acc. Chem. Res.* **1982**, *15*, 40.
(55) Sokolov, V.; Stein, G. *J. Chem. Phys.* **1966**, *44*, 3329.
(56) Boyle, J. W.; Ghormley, J. A.; Hochanadel, C. J.; Riley, J. F. *J. Phys. Chem.* **1969**, *73*, 2886.

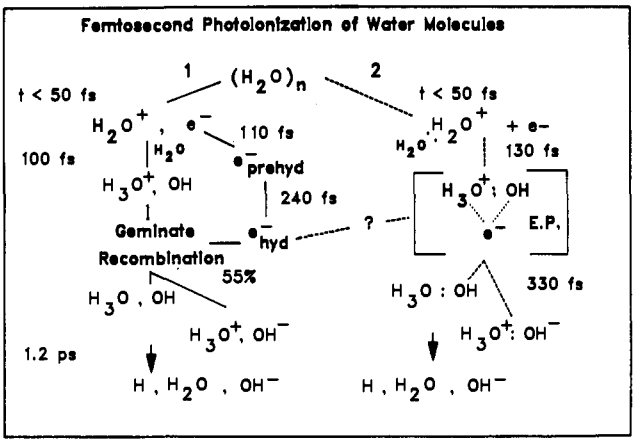

Figure 7. Representation of two photoionization channels in pure liquid water triggered by 100-fs ultraviolet pulses (310 nm). Channel 2 would correspond to a low-energy ionization process yielding an ultrashort lived encounter pair.

clarify several aspects of the physicochemical stage (10^{-15}–10^{-12} s).[44a]

During the initial energy deposition, an instantaneous species absorbing in the near-ultraviolet appears in less than 100 fs. This ultrashort transient absorption has been assigned to the water cation (H_2O^+). Its relaxation would then correspond to the ion–molecule reaction

$$nH_2O + (H_2O^+) \rightarrow (H_3O^+ + OH)_{(n-1)H_2O} \qquad (19)$$

for which the cleavage rate constant has been measured to be 10^{13} s^{-1} at 294 K.[44a] It is important to note that the precursor of the hydronium ion and the hydroxyl radical would relax following an ultrafast proton transfer whose rate constant is faster than the final relaxation step of the trapped electron. This means that a favorable structured environment $(H_3O^+,OH)_{hyd}$ can be created before the electron reaches final equilibrium. This ion–molecule reaction is in agreement with the hypothesis of an autoionization process of water molecules in which the electron undergoes a coupling with neoformed prototropic species on a short spatial range.[57] The cage effect created by this favorable structure will limit the escape of the excess electron far off the water cation (H_2O^+). The early reactivity of this hybrid pair would involve a fast local reorganization of the hydrogen bond lattice without a significant diffusion process and suggest a preeminent role of the ion–molecule reaction to trigger direct electron trapping by siblings. In this hypothesis, if the energy distribution of preexisting traps is determined by solvent fluctuations,[46] it can be suggested that ultrafast structural solvent reorganization initiated by short-lived prototropic species (ion–molecule reaction for instance) would favor the capture of electrons by a new local favorable trap state without the electron undergoing a thermalization process (self-trapping induced by "autoionization" of excited states of water molecules). In this hypothesis, the limiting factor for the formation of the favorable structured environment and the subsequent encounter pair formation $(H_3O^+:e^-:OH)_{hyd}$ would correspond to the activation energy of the reaction involving ultrafast electron transfer from the water cation to nearest surrounding water molecules. The possibility of a cooperative effect between several water molecules (dimer or molecular cluster) remains open as recently suggested by several authors.[58,59]

In conclusion, the important points to be noted from the present study are 2-fold. During the femtosecond photogeneration of an excess electron in pure liquid water at ambient temperature, there is no experimental evidence to consider the existence of an isosbestic point in the near-IR. In this spectral region, a new photochemical channel must be considered through the autoionization of water molecules which yields the formation of an encounter pair between the electron and the neoformed prototropic species $[(H_3O^+:e^-:OH)_{hyd}$ before the total electron hydration process. This nonequilibrium configuration would contribute to the existence of a shoulder in the spectral range 800–900 nm. The deactivation of this electronic hybrid state occurs through a monoexponential process with a cleavage rate constant of 3×10^{12} s^{-1}. The identification of this third nonequilibrium electronic state demonstrates that, at least, two simultaneous electron-transfer channels are involved during the photoejection of epithermal electrons from neutral water molecules. The behavior of the low-threshold ionization process in pure liquid water can lead either (i) to a deactivation process by ultrafast reactivity of non fully hydrated electrons with the hydronium ion or the hydroxyl radical with geminate proton transfer or (ii) to an internal radiationless transition in the vicinity of prototropic entities to yield fully hydrated electrons. In these two cases, the final deactivation process is longer than the internal transition of the infrared presolvated electron to the fully hydrated electron.

Acknowledgment. We gratefully acknowledge the technical assistance of G. Hamoniaux for laser spectroscopy and J. Bottu for data processing.

Registry No. H_3O, 13968-08-6; OH, 3352-57-6.

(57) Han, P.; Bartels, D. M. *J. Phys. Chem.* **1990**, *94*, 5824.

(58) Hameka, H. F.; Robinson, G. W.; Marsden, J. *J. Phys. Chem.* **1987**, *91*, 3150.

(59) Tachikawa, H.; Ogasawara, M. *J. Phys. Chem.* **1990**, *94*, 1746.